

# EXPERIMENTAL AND NUMERICAL INVESTIGATIONS OF FACTORS EFFECT ON THE S-TYPE PITOT TUBE COEFFICIENTS

Woong Kang\*, Nguyen Doan Trang\*\*, Jae Sig Shim\*\*\*, Hee Soo Jang\*\*\* and Yong Moon Choi\*

\* Division of Physical Metrology, Korea Research Institute of Standards and Science  
209 Gajeong-ro, Yuseong-gu, Daejeon 305-340, Korea, ymchoi@kriss.re.kr

\*\*Fluid Flow and Volume Laboratory, Vietnam Metrology Institute  
08 Hoang Quoc Viet, Cau Haiy, Hanoi, Vietnam

\*\*\*Department of Test and Inspection, Korea Environment Corporation  
42 Hawngkyung-ro, Seo-gu, Incheon, 404-170, Korea

## Abstract

In the greenhouse gas emission monitoring from industrial stacks, S-type Pitot tube is the most commonly used to measure the stack gas velocity. Various factors such as Reynolds number, misalignment of installation angle can be additional error sources for the S-type Pitot tube coefficients due to harsh environments. In present study, wind tunnel experiments were conducted to examine the effects of various factors on the S-type Pitot tube coefficients. Numerical simulations were also used to understand flow phenomena around S-type Pitot tube when misalignment and distortion of geometry happen.

## Introduction

Extensive researches for reduction of greenhouse gas emissions have been conducted in the countries with a high proportion of greenhouse gas emissions arising from the energy and industrial fields, such as heavy industry, petrochemical and power plants [1]. In order to reduce greenhouse gas emissions, accurate and reliable studies on greenhouse gas emissions measurement techniques should be carried out first. Recently, the measurement method of greenhouse gas emissions in the world is changing from the fuel consumptions calculation methods of IPCC guidelines to Continuous Emission Monitoring (CEM) used in the U.S. EPA in terms of accurate and actual emission measurements[2,3].

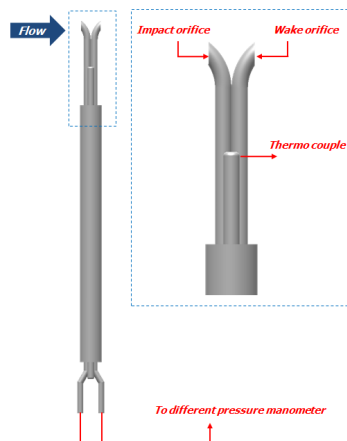


Fig. 1. Configuration of S-type Pitot tube

The average flow rate in the CEM is obtained by measuring an average flow velocity, a density and a cross-section area in the stacks. To measure the flow velocity in the industrial stack, a S-type (Stauscheibe or reverse) Pitot tube have been used widely by ISO standards and EPA Guideline [4-5]. The S-type Pitot tube was designed to measure flow velocity in high dust environments for industrial stacks, which has large pressure orifices and strong tubes compared with the L-type Pitot tube, as shown in figure 1. The flow velocity can be obtained by measuring differential pressure between an impact orifice and an wake orifice based on the Bernoulli equation. The S-type Pitot tube coefficient ( $C_{P,S}$ ) is used to calculate the flow velocity by measuring the the differential pressure with the S-type Pitot tube as the following equation.

$$V = C_{P,S} \sqrt{\frac{2\Delta P}{\rho}} \quad (1)$$

where as  $\Delta P$  is the differential pressure between the impact and the wake orifices.  $\rho$  is the density of fluid in the stacks. The S-type Pitot tube is calibrated in the wind tunnel of the national measurement institutes or the accredited calibration laboratories. However, the S-type Pitot tube is usually installed and inserted in the stacks of harsh environments such as high altitude and high temperature. It is also difficult to observe and check the inside of the stack for the precise installation of the S-type Pitot tube. Therefore, the misalignments such as pitch angle rotation are able to happen during the installation of the S-type Pitot tube outside of the stack. As the diameter of stacks increases, the sampling point positions for measuring velocity distributions in the stack should increase according to EPA method[5]. Since the inserted length of S-type Pitot tube also increases, a yaw angle misalignment of S-type Pitot tube can be caused due to the deflection of the tube in the large diameter stacks. In addition, the flow rate of emission gas can be changed due to unstable process in each industrial condition. This would cause the change of flow velocity (Reynolds number) in the stack, which is measured by S-type Pitot tube. Since S-type Pitot tube is used in different installation alignments and velocity range conditions from calibration conditions, it affects the accuracy of flow rate measurements using calibrated S-type Pitot tube coefficients.

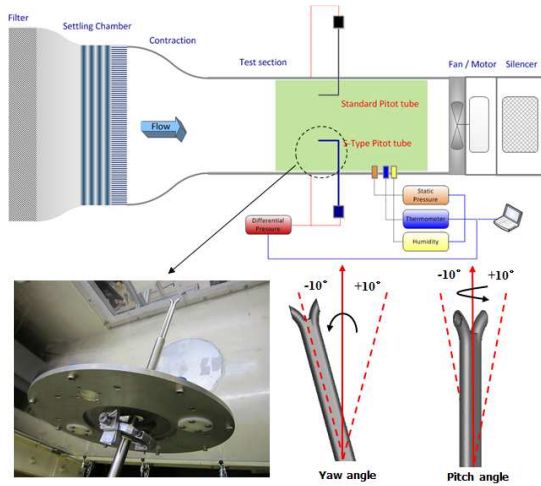


Fig. 2. Experimental set-up of S-type pitot tube in the KRISS wind tunnel

Various attempts have been made to evaluate accuracy of S type Pitot tube coefficients for measuring of flow rate in the stack since the 70s of the last century. Leland et al.[6] examined factors that affect the Pitot tube coefficients, including blockage, misalignment, proximity, turbulence and Reynolds number. Williams and DeJarnette[7] evaluated the effect of geometry changes, misalignments, aerodynamic effects and swirling flows on accuracy of S-type Pitot tube. Vollaro et al.[8] investigated the effect of the impact opening misalignment of S-type Pitot tube which could be deformed by harsh environment of stacks. However, the interval and range of misalignment and Reynolds numbers in the above studies were larger than those of misalignment can occur in the actual measurement environment. Hence, it is not enough to evaluate the uncertainty and accuracy of the flow rate measure by S-type Pitot tube in the stacks. Little attention has been given to explanation why the S-type Pitot tube coefficient changes according to factors such as Reynolds numbers and misalignments.

Recently, several numerical studies have examined to understand flow phenomena around L-type Pitot tube. Boetcher and Sparrow[9] carried out numerical simulations of laminar flow around Pitot tube in the low Reynolds number. They observed the change of streamline pattern due to viscous effects near the nose of the Pitot tube. It caused 2 % deviation of calibration coefficients of Pitot tube. Numerical simulations for averaging Pitot tube have been conducted to understand flow patterns around Pitot tube. Kabacinski and Pospoita[10] designed new cross-section of averaging Pitot tube by using 2D and axi-symmetrical numerical analysis with turbulence model. Calibration method and installation effect of averaging Pitot tubes were also evaluated by numerical studies[11-12]. Despite various numerical studies on L-type Pitot tube and averaging Pitot tube, only few attempts have so far been made to investigate flow fields around S-type Pitot tube numerically[13].

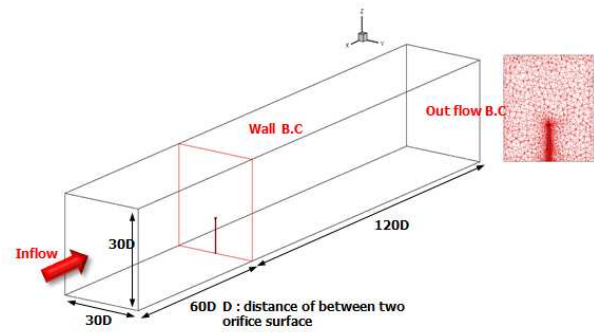


Fig. 3. Computational domain and mesh distribution

The main objective of the present study is to evaluate the effect of various factors such as installation misalignment and Reynolds number on the S-type Pitot tube coefficients for accurate and reliable measurements of greenhouse gas emission in the industrial stacks. To achieve this, wind tunnel experiments in KRISS standard air speed system were conducted to examine the S-type Pitot tube coefficients with various factors condition. Numerical simulations were also used to understand flow phenomena around S-type Pitot tube when misalignment and distortion of geometry happened.

## Experimental apparatus and numerical simulation method

### Experiments in windtunnel

To determine S-type Pitot tube coefficients, calibration tests were performed in subsonic open-circuit wind tunnel of KRISS (Korea Research Institute of Standards and Science), which was used as national air speed standards as shown in figure 2. The test section dimensions were 900 mm(width) × 900 mm(height) × 6000 mm(length). In present experiments, the inlet velocities varied from 2 m/s to 15 m/s. The Reynolds numbers ( $Re_d$ ) defined based on the diameter of static/total pressure orifice are 1,000 ~ 7,000. The turbulent intensity in the test section is less than 0.5%. The expanded uncertainty levels(U) of flow velocity measurements in KRISS wind tunnel standards system are less than 1.1% from 2 - 5m/s and 0.6% 5 - 15 m/s at the 95% confidence level, which was evaluated by ISO/IEC Guide [14-15]. To evaluate the effect of misalignment installation for S-type Pitot tube coefficients, S-type Pitot tube was installed on the wall of test section with a rotating device. The rotating device had been designed to change the pitch and yaw angles of S-type Pitot-tube from  $-10^\circ$  to  $+10^\circ$  with  $2^\circ$  interval. S-type Pitot tubes used in this wind tunnel tests were selected among manufactured products applied to measure the air velocity in the stack.

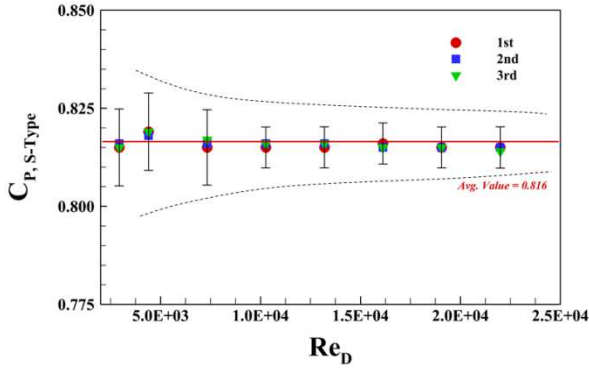


Fig. 4 Reynolds number effect on S-type Pitot tube

## Numerical simulation method

To understand the flow phenomena around the S-type Pitot tube, numerical simulations for three dimensional incompressible Navier-Stokes equations were conducted by using commercial code ADINA 8.7[16]. The finite element method based on Galerkin method was used in the spatial integration of the governing equations. Flow Condition Based Interpolation (FCBI) function was applied as a weighting function to calculate flow fields. The integration was performed with ADINA composite method with second-order accuracy. The turbulence model in present simulations was Detached Eddy Simulation (DES) model developed to solve flow separation and reattachment phenomenon in high Reynolds number [17]. DES is proposed by combining the advantage of Reynolds Averaged Navier-Stokes Simulation (RANS) and Large Eddy Simulation (LES). Length scale is defined as follow in DES with Spalart - Allmaras one-equation model. DES uses Spalart - Allmaras RANS model with low computational cost when length scale equals to length scale in the boundary layer near the wall. On the other hand, LES SGC model was used with high resolution when length scale is in the area away from the walls.

Figure 3 shows the details of computational domain which is identical with test section of wind tunnel,  $30D \times 30D \times 180D$ .  $D$  is the distance between the orifices of static pressure and total pressure. No-slip boundary conditions were used in walls of S-type Pitot tube and the test section of wind tunnel. A pressure out condition is applied as outflow boundary condition. The inflow velocities were varied from 2 to 15 m/s and Reynolds numbers ( $Re_D$ ) were 3,000 - 22,000, respectively. 875,500 unstructured meshes with tetrahedral elements were applied in total computational domain.

## Results and discussion

### The effects of Reynolds numbers on S-type Pitot tube coefficients

The S-type Pitot tube coefficients are determined by comparing the L-type Pitot tube coefficients which are calibrated in the national measurement institutes or the accredited calibration laboratories. In this study, to determine the S-type Pitot tube coefficients, the S-type

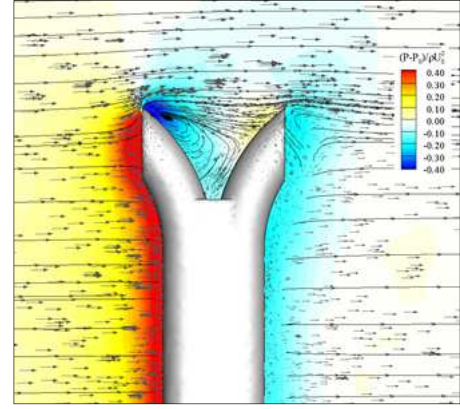


Fig. 5. Pressure distributions and velocity vectors around S-type Pitot tube at  $Re_D=10,000$

and the L-type Pitot tube were installed in the opposite direction of the test section, as shown in Figure 2. The S-type Pitot tube coefficients were calculated by measuring and comparing the differential pressures of two Pitot tubes in each inlet velocity as the following equation.

$$C_{P,S} = C_{P,Std} \times \frac{\Delta P_{Std.}}{\Delta P_S} \quad (2)$$

where  $C_{P,Std}$ ,  $C_{P,S}$  are L-type Pitot tube coefficient and S-type Pitot tube coefficient, respectively.  $\Delta P_{Std.}$ ,  $\Delta P_S$  are differential pressures of the L-type Pitot tube and the S-type Pitot tube.

To investigate the effect of Reynolds numbers on the S-type Pitot tube coefficients, the wind tunnel experiments of S-type pitot tubes were conducted in the range of  $3,000 < Re_D < 22,000$ . The S-type Pitot tube coefficients at each Reynolds number were determined by measuring several times in the same way as the calibration procedure of the national measurement institutes or the calibration laboratories. Figure 4 shows the distribution of the average values and the standard deviations for S-type Pitot tube coefficients over range of the from 3,000 to 22,000. The expanded uncertainty of the S-type Pitot tubes was 1.2%, which is slightly larger than those of L-type Pitot-tube coefficients. The deviation of each value from the average value of S-type Pitot tube coefficients were less than 0.3% within all range of Reynolds numbers. Note that the effect of Reynolds number on the S-type Pitot tube coefficients is negligible compared with the total uncertainty of the flow rate measurements. This result is accordant with those of previous researches on the correction of S-type Pitot tube coefficient [6].

Figure 5 shows the pressure distributions and the velocity vectors around the S-type Pitot tube obtained at  $Re_D=10,000$  by the numerical simulations. The pressure values are normalized by dynamic pressure ( $\rho U_0^2$ ), where  $P_0$ ,  $U_0$  are the upstream pressure and velocity, respectively. High positive pressure distributions are observed near the impact orifice due to the stagnation of incoming flow. On the other hand, negative pressure distributions are presented near the wake orifice since flows are separated from surfaces of the wake orifice. The difference of pressure distribution for the impact and

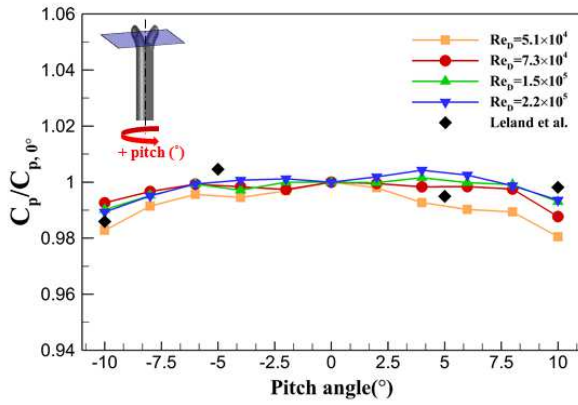


Fig. 6. Effect of pitch angle misalignment on S pitot tube coefficient

wake orifice is calculated to S-type Pitot tube coefficients. Due to complicated geometry between impact and wake orifices, the separated flows are also developed to vortical structure behind the impact orifice. Therefore, the normalized pressure distributions near S-type Pitot tube are observed identically in the range of  $Re_D$  from 3,000 to 22,000, which is consistent with the results of figure 4.

### The effects of misaligned installation on S-type Pitot tube coefficients

The pitch angles of the S-type pitot tube were varied from  $-10^\circ$  to  $+10^\circ$  with  $2^\circ$  interval by using the rotating device installed on the wind tunnel wall. The positive (+) pitch angle is the clockwise direction relative to the installed wall of the test section. Figure 6 shows the change of the S-type Pitot tube coefficients according to the pitch angle misalignments within the range of Reynolds number ( $Re_D$ ) from 5,500 to 22,000. S-type Pitot tube coefficients ( $C_p$ ) at each pitch angle are normalized with S-type Pitot tube coefficients ( $C_{p,0^\circ}$ ) of pitch angle  $0^\circ$ . The normalized S-type Pitot tube coefficients decrease up to -2% as the pitch angle increases to  $\pm 10^\circ$ . Although the fluctuating of S-Pitot tube coefficient can be seen according to the Reynolds number, the symmetric tendency of coefficients in both negative and positive pitch angle appears identically in the all Reynolds numbers.

To further understand the pitch angle misalignments, the flow phenomena around misaligned S-type Pitot tube were investigated by numerical simulations. Figure 7 presents the normalized pressure distribution and the streamline in the cross-section of the S-type Pitot tube, which was cut in the center of two orifices with parallel to the wall of wind tunnel. The flow patterns around the impact and the wake orifices for pitch angle  $-10^\circ$ ,  $0^\circ$  and  $+10^\circ$  at  $Re_D = 10,000$  are compared. In the case of negative pitch angle misalignment, the normalized pressure values near the wake orifice decrease due to the enhancement of separated flow from surface of the orifice. Hence, the difference pressure between impact and wake orifice increases. The S-type Pitot tube coefficients with negative pitch angle show lower value than that of normal installation condition.

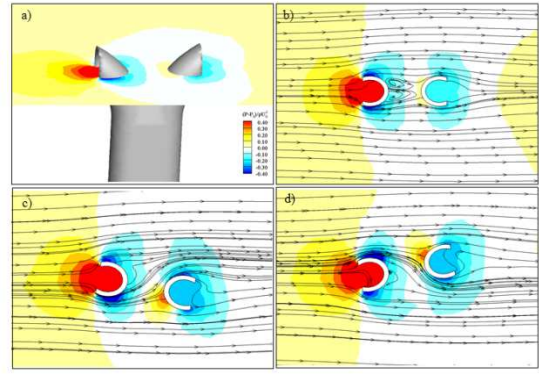


Fig. 7. Pressure distribution and velocity vector with misalignment installation according to pitch angle, a) cross-sections of S-type Pitot tube, b) Pitch angle  $=0^\circ$ , c) Pitch angle  $=-10^\circ$ , d) Pitch angle  $=+10^\circ$

In the case of positive pitch angle misalignment, since the direction of incoming and separating flow near two orifices is symmetric with that of negative pitch angle misalignment, the S-type Pitot tube coefficients show similar tendency according to pitch angles to values of negative pitch angle.

To investigate the effect of yaw angle misalignments due to the deflection of the S-type Pitot tube in the large diameter stacks, wind tunnel experiments were conducted in the range of yaw angles from  $-10^\circ$  to  $+10^\circ$  with  $2^\circ$  interval. The positive yaw angle is the downstream direction of flows in the test section. Figure 8 represents the change of the S-type Pitot tube coefficients regarding to the yaw angle misalignments within the range of from 5,500 to 22,000. The normalized S-type Pitot tube coefficients decrease up to -2% regardless of Reynolds numbers as the yaw angle increases to  $-10^\circ$  in the negative direction. In the case of positive yaw angles, the S-type Pitot tube coefficients increase as Reynolds numbers and yaw angles increase. To further explore the change of the S-type Pitot tube coefficients according to the yaw angle misalignments, numerical simulation for flow fields around the misaligned S-type Pitot tube were conducted at  $Re_D = 10,000$ , as shown in figure 9. In the case of  $-10^\circ$  yaw angle, the low pressure distributions are observed near the wake orifice since a vertical structure grows up behind the wake orifice. Hence, the S-type Pitot tube coefficients decrease in the negative yaw angles.

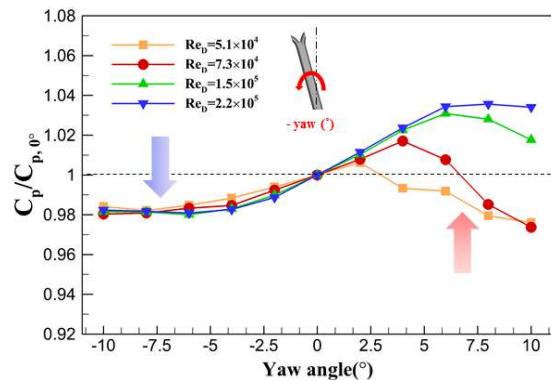


Fig. 8. Effect yaw angle misalignment on S pitot tube coefficient

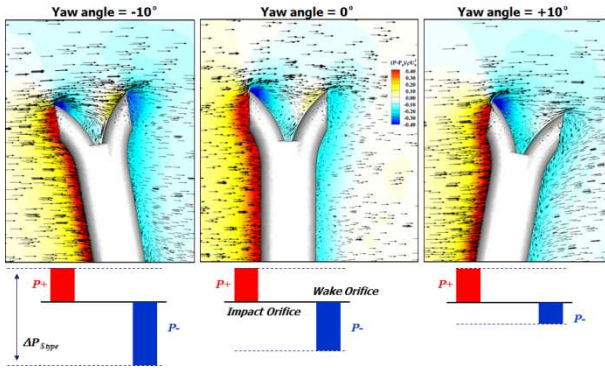


Fig. 9. Pressure distribution and velocity vector with misalignment installation according to yaw angle

On the other hand, when the positive yaw angle misalignments happen, incoming flows separate strongly at the upper edge of the impact orifice due to the tilted geometry. Therefore, the S-type Pitot tube coefficients increase due to the recovery of the pressure distribution near the wake orifice. Note that the maximum deviation of the S-type Pitot tube coefficient is about 2 % in the negative yaw angle misalignments which can occur in the industry stacks due to the deflection of the S-type Pitot tube.

## Conclusion

For the reduction of greenhouse gas emission as national policies about global warming, it is essential to develop accurate and reliable measurement techniques for greenhouse gas flow rate. To this end, experimental and numerical studies were conducted on the factors that affect the accuracy of flow rate measurements by using the S-type Pitot tube which used in the field of industry, energy and plant etc. The effect of Reynolds numbers, misaligned installations and manufacturing qualities on the S-type Pitot tube coefficients were investigated by considering the flow rate measurement environments in the industrial stacks. Conclusions about the change of S-type Pitot tube coefficients by the factors investigated in the present study are as follows.

The deviation and uncertainty of S-type Pitot tube coefficients in range of  $3,000 < Re_D < 22,000$  were less than 0.3 % and 1.21 %, respectively. Hence, the change of Reynolds numbers has no effect on the S-type Pitot tube coefficients. The S-type Pitot tube coefficients decreased up to -2% as the pitch angle misalignments happen from  $-10^\circ$  to  $+10^\circ$ . The symmetric tendency of the S-type Pitot tube coefficients in both positive and negative pitch angle misalignments were revealed by numerical simulation of flow phenomena near the impact and wake orifices of S-type Pitot tube. The maximum deviation of the S-type Pitot coefficient is about -2% in the negative yaw angle misalignments which can occur in the industry stacks due to the deflection of the S-type Pitot tube. The flow structures near the impact and wake orifices with numerical simulations explained the change of S-type Pitot tube coefficients according to the direction of yaw angle misalignments.

## References

- [1] M. Granovskii, I. Dincer and M.A. Rosen, "Greenhouse gas emissions reduction by use of wind and solar energies for hydrogen and electricity production : Economic factors", International Journal of Hydrogen Energy , Vol. 32, pp. 927-931, 2006.
- [2] IPCC, "Guidelines for National Greenhouse Gas Inventories", International Panel on Climate Change, 2006
- [3] EPA, "Continuous Emission Monitoring", U.S. Environmental Protection Agency, Title 4, Part 75 Appendix F, 1993.
- [4] ISO, "Stationary source emission –Measurement of velocity and volume flow rate of gas streams in ducts", International Standard Organization 10780, 1994.
- [5] EPA, "Determination of stack gas velocity and volumetric flow rate (Type S Pitot tube)", U.S. Environmental Protection Agency, Part 60 Appendix A, Method 2, 1971.
- [6] B.J. Leland, J.L. Hall, A.W. Joensen and J.M. Carroll, "Correction of S-type pitot-static tube coefficient when used for isokinetic sampling from stationary source", Environment Science and Technology, Vol. 11(7), pp. 694-670, 1977.
- [7] J.C. Willams and F.R. DeJarnett, "A study on the accuracy of type-S Pitot tube", EPA-600/4-77-030, 1977.
- [8] R.F. Vollaro, "Guidelines for S type Pitot tube calibration", U.S. Environmental Protection Agency EPA-450/2-78-042b, 1978.
- [9] S.K.S Boetcher and E.M. Sparrow, "Limitations of the standard Bernoulli equation method for evaluating Pitot/impact tube data", International Journal of Heat and Mass Transfer, Vol. 50, pp.782-788, 2007.
- [10] M. Kabacinski and J. Pospolita, "Numerical and experimental research on new cross-sections of averaging Pitot tubes", Flow Measurement and Instrumentation, Vol. 19, pp. 17-27, 2008.
- [11] D. Weceł, T. Chmielniak and J.M. Kotowicz, " Experimental and numerical investigations of the averaging Pitot tube and analysis of installation effects on the flow coefficient", Flow Measurement and Instrumentation, Vol. 19, pp.301-306, 2008.
- [12] V. Vinod, T. Chandran, G. Padmakumar and K. K. Rajan, "Calibration of an averaging pitot tube by numerical simulations", Flow Measurement and Instrumentation, Vol. 24, pp.26-28, 2012.
- [13] N. D. Trang, W. Kang, J. S. Shim, H.S. Jang, S.M. Park and Y.M. Choi, "Experimental study of the factors effect on the S type Pitot tube coefficient", XX IMEKO World Congress, 2012.
- [14] ISO, "Guide to the expression of uncertainty in measurement", ISO guide 25, 1993.
- [15] ISO, "Measurement of fluid flow – Procedure for evaluation of uncertainty", International Standard Organization 5168, 2005
- [16] ADINA R & D Inc, "ADINA Theory an modeling guide Vol III : ADINA CFD & FSI ", Report ARD 12-10, 2012.
- [17] P.R. Spalart and S.R. Allmaras, "A one equation turbulence model for aerodynamic flows", La Recherche Aerospatiale, Vol. 1, pp.5-21, 1994.